Journal of Applied Fluid Mechanics, Vol. 12, No. 1, pp. 281-291, 2019.
Available online at www.jafmonline.net, ISSN 1735-3572, EISSN 1735-3645.
DOI: 10.29252/jafm.75.253.29026

Effect of the Heating Block Position on Natural Convection in a Three-Dimensional Cavity Filled with Nanofluids

M. Sannad†, B. Abourida, L. Belarche, H. Doghmi and M. Ouzaouit

National School of Applied Sciences, Ibn Zohr University, Agadir, BP 1136, Morocco

†*Corresponding Author Email: mohamedsannad@gmail.com*

(Received March 19, 2018; accepted August 25, 2018)

ABSTRACT

This paper consists on a three-dimensional numerical approach of natural convection in a cavity containing the nanofluid. The cavity contains an isothermal heating block in the middle of the bottom (case BH) and the top (case TH) walls and kept at a hot temperature T_H. The right and the left vertical walls of the cavity are kept at a cold temperature Tc. The study's parameters are: the volume fraction Φ varying between 0 and 0.03, and the Rayleigh number $10^3 \leq Ra \leq 10^5$. The considered nanofluid is water + Cu. The results illustrate that the Rayleigh number Ra and the volume fraction Φ have a positive effect and they also improve the heat transfer. Interesting results have also been found while comparing the two considered configurations.

Keywords: Natural convection; Nanofluids; Heating block; Heat transfer.

NOMENCLATURE

C_p	specific heat
g	gravitational acceleration
k	thermal conductivity
Nu	Nusselt number
Nu_a	average Nusselt number
p	pressure
P	non dimensional pressure
Pr	Prandtl number of water
Ra	Rayleigh number
T	temperature
u,v,w	dimensional velocities
U,V,W	dimensionless velocities
x, y, z	dimensional coordinates
X,Y,Z	non Dimensionle Cartesian coordinates
α	thermal diffusivity
β	volumetric thermal expansion coefficient
θ	non-dimensional temperature
μ	dynamical viscosity
ν	kinematic viscosity
ρ	density
Φ	volumic fraction

Subscripts

a	average
C	cold
f	fluid (pure water)
H	hot
HC	horizontal cavity
nf	nanofluid
np	nanoparticles

1. INTRODUCTION

Much attention has been drawn by natural convection heat transfer phenomena as it has a broad range of engineering applications such as heat exchangers, solar collectors, electronic cooling and thermal storage systems. However, the conventional fluid used, such as water, oil, and ethylene glycol has very low thermal conductivity which is an obstacle on the way of innovations in thermal management and energy efficiency.

In order to improve the heat transfer by convection in these applications, the researchers started looking deeper into the structure of the matter at the molecular level which has given birth to the development of nanofluids that was introduced by Choi (1995), who defined them as liquid-solid mixtures which consist of non-metallic or metallic nanometric size solid particle's and base liquid.

Putra *et al.* (2003) have studied experimentally the behavior of nanofluids such as (Al_2O_3-water) and (CuO-water) inside a horizontal cylinder submitted to constant temperatures. They detected that the heat transfer increases when the concentration of nanoparticles increases and becomes more

significant for nanofluid (CuO-water). The numerical study of Mahmoudi (2010) also reported similar heat transfer improvement in L-shaped cavities.

Ho *et al.* (2010) have studied experimentally the Al_2O_3-Water nanofluid natural convection in the Speakers Square, and they consider three different sizes of those. They also measured the nanofluid thermophysical properties in order to explain the unusual increase or decrease of the heat transfer. They have found that these variations cannot be explained solely by the nanofluide thermophysical properties, but also by other factors such as the transport mechanisms that modify the homogeneity of the nanoparticles volume fraction in the enclosure.

In the last years, there are a substantial number of numerical studies on nanofluid convective heat transfer in enclosures. For example, Khanafer *et al.* (2003) studied digitally the natural convection in nanofluids. They used respectively Brinkman model and thermal dispersion model for viscosity and thermal conductivity. Their results illustrated that at any Grashof number, the suspended nanoparticles substantially augment the heat transfer rate. The studies of Jou *et al.* (2006), Hwang *et al.* (2007), Ho *et al.* (2008), Santra *et al.* (2008) and Abu Nada *et al.* (2009) demonstrated that the heat transfer is much important when they increase the volume fraction.

Oztop *et al.* (2008) dealt with digitally the natural convection in the rectangular enclosures partially heated. They analyzed the effect of the nature of nanoparticles, the volumetric concentration, Rayleigh number, the position and the length of the heat source and the enclosure's aspect ratio.

Further, the Nusselt number increases linearly with the solid concentration of the nanofluid. A similar results have been established by Ravink *et al.* (2010) who showed that the heat transfer is significantly enhanced by the increase of the volumic fraction of the nanofluid. This improvement is obvious, compared to the base fluid (pure water) and also in the case of dominant conduction heat transfer.

Sheikhzadeh *et al.* (2013) have studied the effects of the mechanisms of transport of nanoparticles Al_2O_3 on the natural convection laminar in a square enclosure; their results have shown that the transport model is in good agreement with experiment, unlike the homogeneous model. Khaled Khodary Esmaeil. (2015) Has investigated numerically the natural convection of nanofluides inside a heated cavity. They assess the effects of the use of different thermal conductivity models and the nanofluids dynamic viscosity on the performance of heat transfer. It was found that the heat transfer efficiency depends strongly on the nanofluide viscosity, whereas the role of the thermal conductivity is considered as secondary.

Sannad *et al.* (2016), have studied numerically the nanofluid convective heat transfer in a 3D cubical cavity heated by two portions on its vertical wall. The obtained results showed the important effect of some parameters such as, the volume fraction, the nanoparticles type and the Rayleigh number. Hence, the increase of Rayleigh number leads to a large improvement of heat transfer evacuated across the cavity. Similarly, the increase of the volume fraction causes an enhancement of the flow and thermal exchanges. In addition, the resulting heat transfer for Cu nanoparticles is higher than that obtained with TiO_2, and Al_2O_3.

The same models as those used by Guiet *et al.* (2012), are examined the effects of the solid concentration of the nanoparticles, and the heat source position on the heat transfer . this results demonstrates that the heat transfer and flow are considerably affected by the heating source's size, where if they increased the size, they observed an increases of the Nu_a.

However, most of these available practical and theoretical works, conducted on this subject, they considered the case of 2D free convection while the three-dimensional approach allows a better and more realistic simulation of the heat transfer and fluid flow in the enclosure. Hence, the object of the this investigation is to study numerically the laminar natural convection in a cubical enclosure, the cavity contains an isothermal heating block filled with nanofluid. The temperature distributions, the velocity patterns and the heat transfer rates are analyzed and discussed in this paper.

2. PROBLEM FORMULATION

Figure 1 illustrate studied configurations . The first configuration (case BH) consists of a 3D cubical cavity with the right and the left vertical walls kept at a cold temperature T_C, while the top wall is kept at a hot temperature T_h. The cavity contains an isothermal heating block in the middle of the bottom wall. In the other case (TH), the isothermal heating block is located in the middle of the top wall while the bottom wall is kept at a the heating temperature T_h. The others parties of the walls that contains the block are adiabatic. The effect of the heated block's position on the heat transfer and fluid motion is studied in this paper.

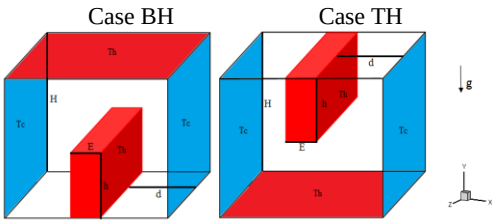

Fig. 1. Studied configurations and coordinates.

We discretized our governing equations by finite volume method, and we have adopted the Boussinesq approximation, also neglected the viscous dissipation.

The physical parameters are given by the next formulas:

The density:

Table 1 Thermophysical properties of pure water and nanoparticle's

	ρ (kg.m^{-3})	β (K^{-1})	k (W.m^{-1}.K^{-1})	C_p (J.kg^{-1}.K^{-1})
Pure Water	997.1	21x10^{-5}	0.613	4179
AL_2O_3	3970	0.85x10^{-5}	40	765
Cu	8933	1.67x10^{-5}	400	385
TiO_2	4250	0.90x10^{-5}	8.9538	686.2

In order to estimate the volumetric mass density, we supposed that the mixture is perfectly homogeneous (good dispersion of nanoparticle's in base fluid), in term of volume fraction Φ at a defined temperature T. In our case, we use the commune definition of volumetric mass density in a mixed phase:

$$\rho_{nf} = \left(\frac{m}{v}\right)_{nf} = \frac{m_f + m_s}{v_f + v_s} = \frac{\rho_f v_f + \rho_s v_s}{v_s + v_f}$$

ρ_{nf}, ρ_f and ρ_s are respectively the density of the nanofluid, the pure water and the solid nanoparticles.

Nanoparticule's volume fraction marked as Φ designs the report between the nanoparticle's volume and the total volume (base fluid + nanoparticles).

$$\phi = \frac{v_s}{v_f + v_s}$$

The nanofluid's density is given by:

$$\rho_{nf} = (1-\phi)\rho_f + \phi\rho_{np} \quad (1)$$

The heat capacitance of the nanofluid:

$$(\rho C_p)_{nf} = (1-\phi)(\rho C_p)_f + \phi(\rho C_p)_{np} \quad (2)$$

The nanofluid thermal expansion coefficient:

$$\beta_{nf} = (1-\phi)\beta_f + \phi\beta_{np} \quad (3)$$

The nanofluid's dynamic viscosity:

It's given by Brinkman (2005) who has developed the Einstein formula to cover a wide range of volumetric concentrations.

$$\mu_{nf} = \frac{\mu_f}{(1-\phi)^{2.5}} \quad (4)$$

The thermal diffusivity of nanofluids:

$$\alpha_{nf} = \frac{k_{nf}}{(\rho C_p)_{nf}} \quad (5)$$

The effective thermal conductivity of nanofluids is given by Maxwell (1881) as follows:

$$\frac{k_{nf}}{k_f} = \frac{k_{np} + 2k_f - \left[2(k_f - k_{np})\phi\right]}{k_{np} + 2k_f + \left[\phi(k_f - k_{np})\right]} \quad (6)$$

k_f, k_{nf} and k_{np} are respectively the thermal conductivities of the base fluid, the nanofluid and the solid nanoparticles.

Hence, the obtained dimensionless governing equations are:

$$\frac{\partial U}{\partial X} + \frac{\partial U}{\partial Y} + \frac{\partial U}{\partial Z} = 0 \quad (7)$$

$$U\frac{\partial U}{\partial X} + V\frac{\partial U}{\partial Y} + W\frac{\partial U}{\partial Z} = -\frac{\partial P}{\partial X} + \frac{\mu_{nf}}{\alpha_f \rho_{nf}}\left(\frac{\partial^2 U}{\partial X^2} + \frac{\partial^2 U}{\partial Y^2} + \frac{\partial^2 U}{\partial Z^2}\right) \quad (8)$$

$$U\frac{\partial V}{\partial X} + V\frac{\partial V}{\partial Y} + W\frac{\partial V}{\partial Z} = -\frac{\partial P}{\partial Y} + R_a * P_r * \theta * \frac{\rho_f \beta_{nf}}{\rho_{nf}\beta_f} + \frac{\mu_{nf}}{\alpha_f \rho_{nf}}\left(\frac{\partial^2 V}{\partial X^2} + \frac{\partial^2 V}{\partial Y^2} + \frac{\partial^2 V}{\partial Z^2}\right) \quad (9)$$

$$U\frac{\partial W}{\partial X} + V\frac{\partial W}{\partial Y} + W\frac{\partial W}{\partial Z} = -\frac{\partial P}{\partial Z} + \frac{\mu_{nf}}{\alpha_f \rho_{nf}}\left(\frac{\partial^2 W}{\partial X^2} + \frac{\partial^2 W}{\partial Y^2} + \frac{\partial^2 W}{\partial Z^2}\right) \quad (10)$$

$$U\frac{\partial \theta}{\partial X} + V\frac{\partial \theta}{\partial Y} + W\frac{\partial \theta}{\partial Z} = \frac{\alpha_{nf}}{\alpha_f}\left(\frac{\partial^2 \theta}{\partial X^2} + \frac{\partial^2 \theta}{\partial Y^2} + \frac{\partial^2 \theta}{\partial Z^2}\right) \quad (11)$$

All of the above variables have been dimensionless based on the following definitions:

$$(X, Y, Z) = \frac{(x, y, z)}{L_{ref}} \quad (12)$$

$$(U, V, W) = \frac{(u, v, w)}{V_{ref}} \quad (13)$$

$$P = \frac{p + \rho_0 g y}{P_{ref}} \quad (14)$$

$$\theta = \frac{T - T_F}{\Delta T_{ref}} \quad (15)$$

The adopted boundary conditions are:

$\frac{\partial \theta}{\partial n} = 0$ On the adiabatic walls

Where n is the normal to the considered wall.

For the BH configuration:

$\theta = -0.5$, for $X = 1$, $X = 0$; on the cold walls

$\theta = 0.5$, on the heated block

$\theta = 0.5$, for Y=1; on the heating wall

For the TH configuration:

$\theta = -0.5$, for $X = 1$, $X = 0$; on the cold walls

$\theta = 0.5$, on the heated block

$\theta = 0.5$, for Y=0; on the heating wall

The adopted hydrodynamic boundary conditions are:

$U = V = W = 0$ For all walls.

The local Nusselt number is defined as:

$$Nu_l(Y,Z) = \frac{k_{nf}}{k_f}\frac{\partial\theta}{\partial X} \tag{12}$$

The average Nusselt number, Nu_a, is defined as the integral of the temperature flux through the horizontal and vertical walls are formulated as:

$$Nu_{a_H} = \frac{k_{nf}}{k_f}\int_{S_H}\frac{\partial\theta}{\partial Y}dXdZ$$
$$Nu_{a_V} = \frac{k_{nf}}{k_f}\int_{S_V}\frac{\partial\theta}{\partial X}dYdZ \tag{13}$$

With S_H and S_V are respectively horizontal and vertical surfaces.

3. NUMERICAL METHOD

We discretized our governing equations by finite volume method, we have considered the boussinesq approximation and also neglected the viscous dissipation. To overcome the difficulty associated with the determination of the pressure, the SIMPLEC algorithm is used to solve the momentum equations coupled with the continuity one. The Alternating Direction Implicit scheme (ADI) is then adopted to solve the algebraic discretized equations .The obtained numerical code was validated by comparing its results with those of Ravnik *et al.* (2010) (Fig. 2) and Lo *et al.* (2007) (Tables 2 and 3).

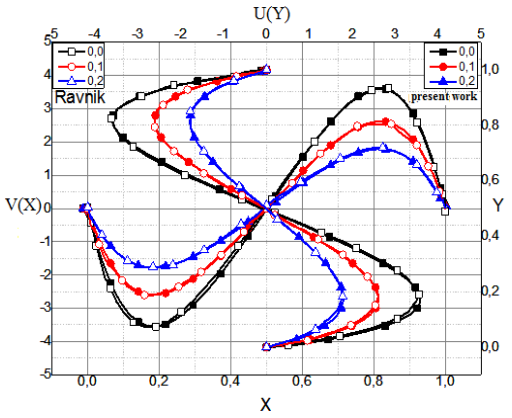

Fig. 2. Comparison of the velocity V(X) and U(Y) between our results and those of Ravnik *et al.* (2010).

Table 2 Comparison of the Nu_a between our results and those of Lo *et al.* (2007)

	Lo *et al.* (2007)	Our study	Relative gap
Ra =10^3	1.0710	1.0770	0.56%
Ra =10^4	2.0537	2.0932	1.9%
Ra =10^5	4.3329	4.4329	2.3%
Ra =10^6	8.6678	8.8997	2.6%

Table 3 Numerical results for Ra=10^3 in the case of horizontal cavity (HC)

Ra=10^3 and (HC)		Lo *et al.* (2007)	Our study	
U_{MAX}	X	3.5227	0.0000	0.00000
	Y		0.1956	0.17796
	Z		0.5000	0.49999
V_{MAX}	X	3.5163	0.3044	0.33170
	Y		0.5000	0.48305
	Z		0.5000	0.49999
W_{MAX}	X	0.1726	0.0000	0.00000
	Y		0.5000	0.49999
	Z		0.2500	0.73728

In order to validate our code, we compared our results with the studies conducted by Lo *et al* and Ravnik *et al*. as presented in above, We can notice that our results are in good agreement with these studies.

4. RESULTS

In this study, we conducted a numerical approach in order to study the effects of the heating conditions on the natural convection in an enclosure containing the nanofluid. The Prandtl number of water is equal to 6.2 and the nanoparticle's volume fraction is $0 \le \Phi \le 0.03$. We consider one type of nanoparticles in this work: Cu. Its properties are listed in Table 1. The range of Rayleigh number is $10^3 \le Ra \le 10^5$. We present in this part the isotherms for different nanoparticles, values of the volume fraction and the Rayleigh number. Also the speed variations and the resulting Nusselt number are presented.

In order to visualize the temperature distribution within the studied cavity, 3D isotherms for (Cu+Water) are showed in Fig. 3, for the two considered configurations (BH and TH), Ra=10^3, 10^4 and 10^5 and Φ = 0.03. For Ra = 10^3, the isotherms are parallel to the actives walls in the majority of the cavity, which means that conduction is the dominating mode of heat transfer. We also observed that the increase of the Rayleigh number is accompanied with an increase of the flow intensity. The convective effects improve then considerably the heat transfer. Consequently, the isotherms change completely their shape for Ra = 10^5.

The isotherms also show that the temperature of the closest fluid to the upper heat block (case BH) is greater than that of the fluid adjacent to the lower

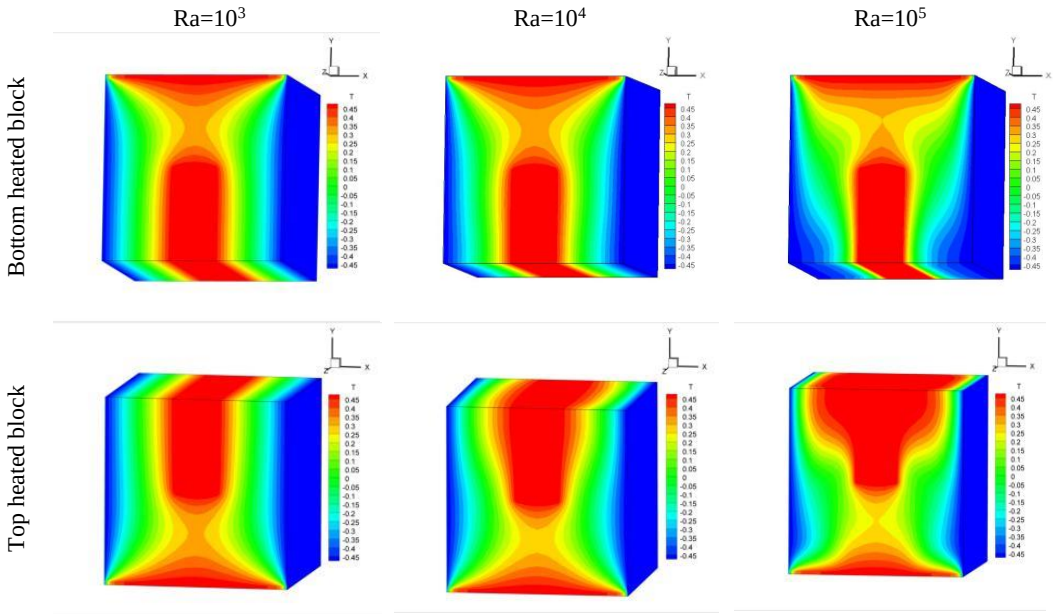

Fig. 3. 3D isotherms for the two configurations (BH and TH), Φ = 0.03, different Ra and for (Cu+Water).

heat block (case TH). This is due to the course followed by the fluid. Indeed, the cold fluid descending from the right wall gets in touch with the lower heat block, before reaching the upper one, which is obvious because the fluid always move from hot areas to cold areas.

The isotherms also show that the fluid's temperature change's with the augmentation of the Rayleigh number, for Ra = 10^3, the fluid's temperature which is near the top block and near the left wall is about 0.45, but for Ra = 10^5, the temperature decreases to 0.2. Because for the low value of Ra, the dominant transfer mode is conduction, and the speed of circulation of the fluid is low compared to that in the case of convection, while the fluid remains in contact with the block during a very long duration which gives a significant rise in temperature compared to the case of convection.

The fluid motion leads the heat from the active areas through the cavity. High values of the temperature are normally observed in the top part of the enclosure and near the block as shown by the corresponding isotherms.

For more visibility of the fluid motion and heat transfer, isotherms are presented at the mid-planes of the cavity. Figure 4 shows the temperature contours on the X, Y, and Z planes for different Rayleigh number values (case BH). Further isotherms were produced for different plans in the cavity, and presenting symmetry relative to the center of the cavity for the considered planes (X and Z).

For low values of Ra (Ra= 10^3), we can notice a slight distortion of the isotherms in all the presented cases, characterizing the appearance of the convective regime within the cavity. The increase of Ra leads to a better heat transfer from the heating block to the cold walls as shown the corresponding isotherms. This effect is noticed for all the considered planes. Hence, the plane Z = 0.5 was chosen for the following presentations. In addition, it presents a perfect symmetry (compared to the planes Z = 0.04, Z = 0.27, Z = 0.72 and Z=0.9).

In this section, we consider the case where the cavity is filled with water and other solid nanoparticle, Cu. The volume fraction solid is varied from 0% to 3%.

Figure 5 shows the temperature fields in the case of pure water and the mixture (water + Cu) for Φ = 0.03 and different Rayleigh numbers. It is clear from this figure that the pure water and the mixture have the same thermal behavior. The thermal field is marked by a horizontal stratification within the cavity and by strong thermal gradients on the active walls, which means that the heat transfer is largely convective.

It is also seen from the figure that when the heat source is located at the top wall of the cavity (case TH), the isotherms show strong thermal gradients on all sides of the cavity, in comparison with the other configuration's one.

Figure 6 shows the Streamlines for the pure water and the water+Cu, Φ = 0.03 and three Rayleigh numbers values (Ra = 10^3; 10^4; 10^5). The heat block located in the middle of the cavity for the both cases (BH and TH). The figure clearly shows that for all the Rayleigh numbers, the structure of the flow is characterized by the presence of two cells occupying almost the entire cavity. Further flow presentations were produced for plan Z=0.5 in the cavity, and show that the flow consists of two cells, turning clockwise and presenting a symmetry relative to the center of the cavity for the plane X=0,5.

When the Rayleigh number increases, the buoyancy force becomes large, and therefore the maximum stream function of the pure fluid and the nanofluid

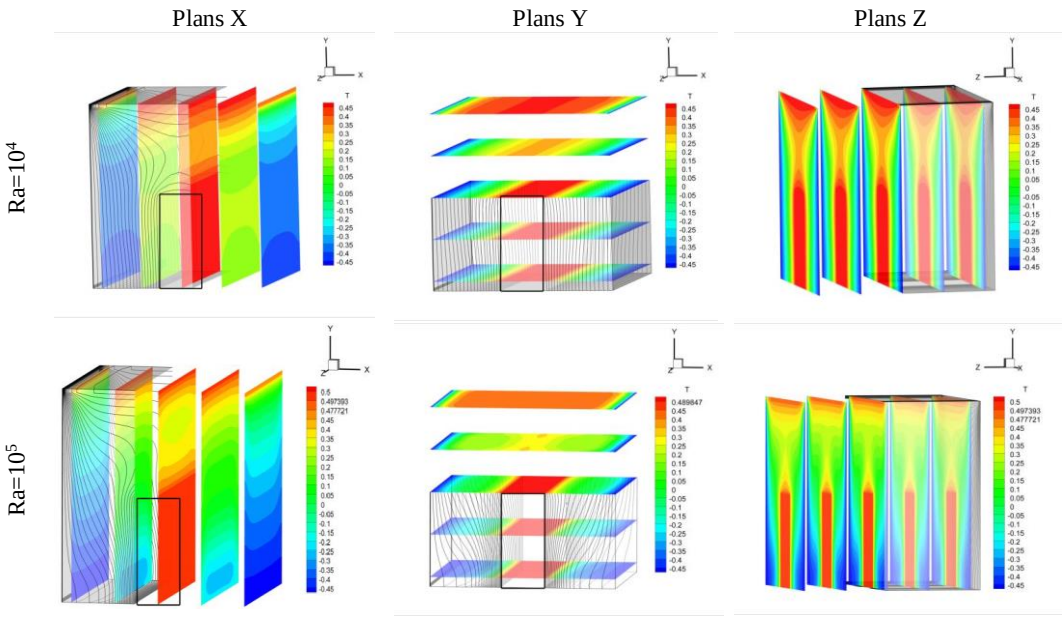

Fig. 4. The isotherms for water+Cu for different plans, and different Ra with Φ = 0.03 (Case BH).

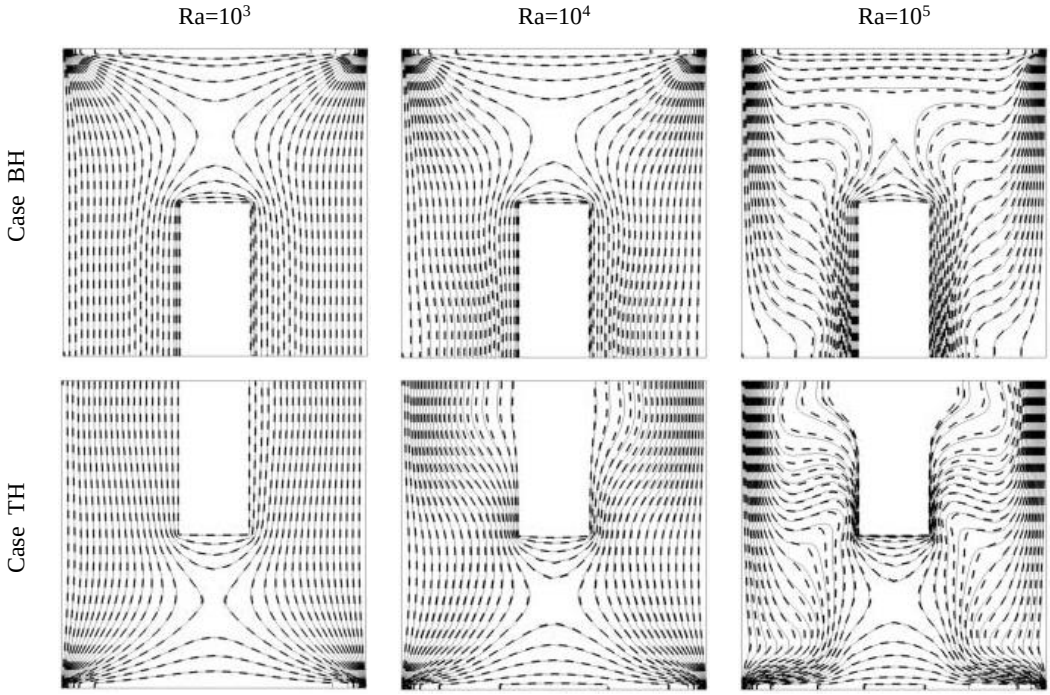

Fig. 5. Isotherms in the plan Z=0.5, for pure water and water+Cu for different Ra with Φ = 0.0, 0.03.

increases. These values show also that the flow in the presence of nanofluid is stronger than that in the case the pure fluid for Ra greater than 10^4.

Whereas for Ra≤10^4, the flow of pure fluid becomes stronger. This behavior is due to the viscosity (resistance to the flow) and also to the Archimede's force which the density depends on.

In the case of low Rayleigh numbers, the driving force decreases for the pure fluid and the nanofluid, and it is the viscosity which determines the intensity of the convection motion. For this reason the pure fluid which has the greatest intensity. On the contrary, for large Rayleigh numbers, the buoyancy force becomes more important and it is the nanofluid that circulates faster. The shape of the isotherms shows a change in the heat transfer mode and practically in the convection mode, because the effect of the viscosity can only be observed when there is a flow, this is the case of convection. As the Ra increases, the heat transfer mode changes from conduction to convection. At Ra = 10^5, the thermal field is marked by a horizontal stratification inside the cavity and by strong thermal gradients on the

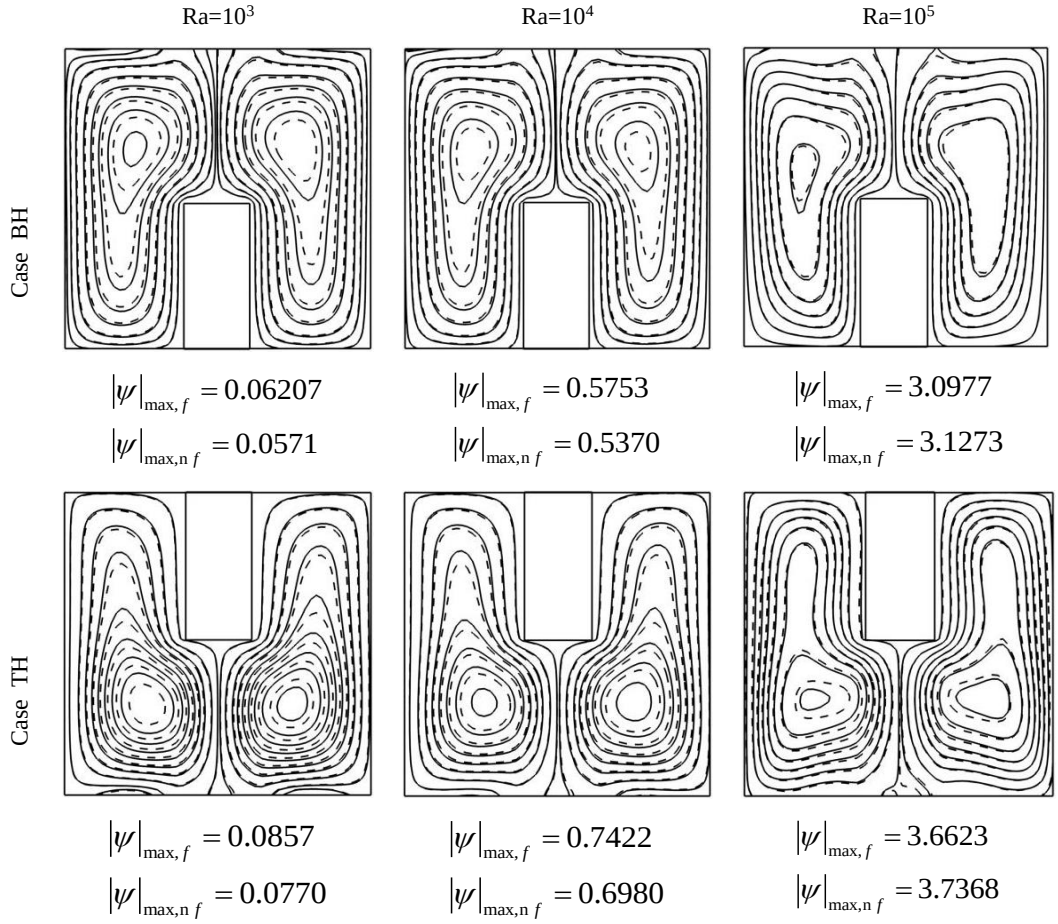

Fig. 6. Streamlines contours in the plan Z=0.5, for pure water and water+Cu for different Ra with Φ = 0.0, 0.03.

We have for Figs. 5 and 6:
pure water (—————)
water+Cu (---- - - - - -)

active walls, which means that the heat transfer is mainly dominated by convection.

From all the previous results, we can conclude that the optimum configuration from the thermal and dynamic point of view is the one with the heat source located on the top wall (case TH). This position is the optimal choice in order to obtain the best heat transfer, because the thermal and dynamical transfers are influenced by the value of the buoyancy force which is favorable in the case of the configuration (TH).

The profile of the vertical components of the flow velocity V (X) and U (Y) along the horizontal median plan of the enclosure for Ra=10^3, 10^4 and 10^5; Φ =0.0 and 0.03 is shown in Figs. 7 and 8 respectively for the configurations BH and TH.

The figures make it possible to understand the behavior of the flow in the enclosure. The profile shows that the cell formed inside the enclosure circulates in a clockwise direction. When we increase the Rayleigh number, the maximum vertical velocity increases by the effect of the buoyancy force.

For U (Y), the flow becomes almost stagnant at the position Y = 0.5 for the case BH configuration. However, in the case of TH configuration, the flow keeps the same shape from Y = 0.5 to 1 because of the existence of the block is in the center of the cavity.

For Ra=10^3, we observe that the pure water reaches the highest values of velocities, but when we add solid particles the flow slows down. And when The

velocity decrease, the convective heat transfer also decrease.

However, since in this regime the majority of heat is transported by conduction, the decrease of nanofluid's velocity is negligible, because the overall heat transfer of nanofluids is better than that of water, which is due to the higher thermal conductivity of a nanofluid.

In the Ra=10^5 case convection dominates. We also noticed that nanofluids velocities are higher than the those the pure water. Thus, using nanofluids,

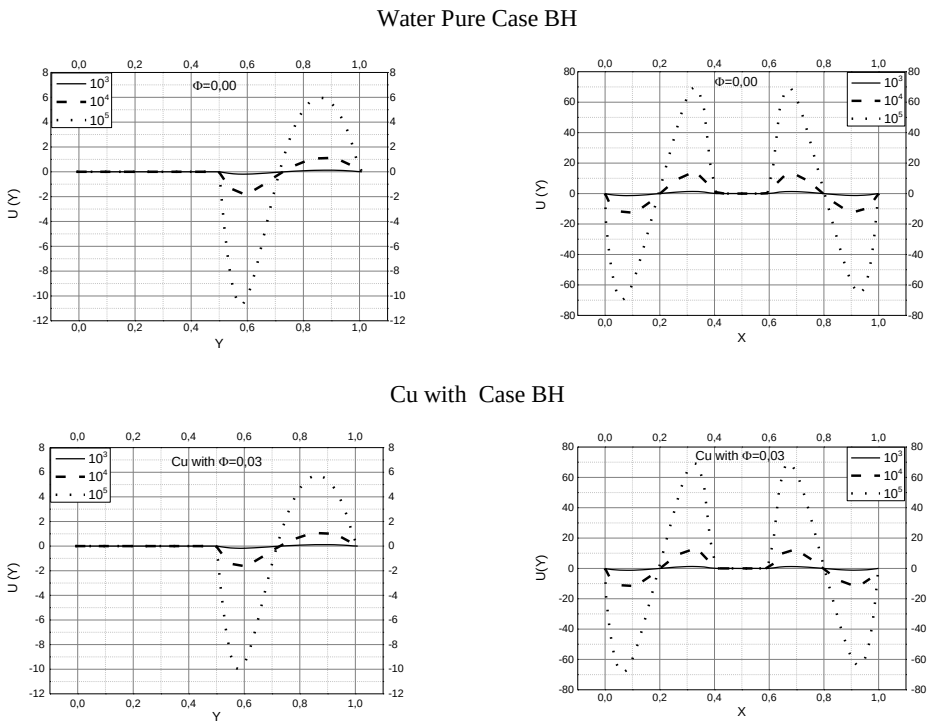

Fig. 7. Profiles of velocity V (X) and U (Y) of the nanofluids in the central plane Z=0.5 for different values of Φ and Ra (Case BH).

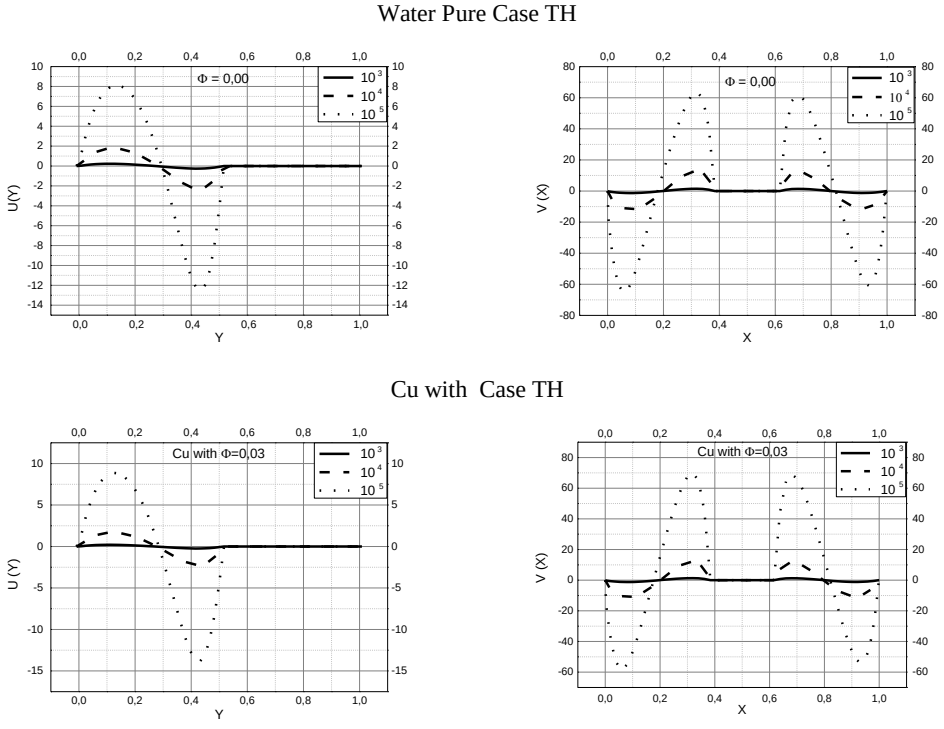

Fig. 8. Profiles of velocity V (X) and U (Y) of the nanofluids in the central plane Z=0.5 for different values of Φ and Ra (Case TH).

modify the velocity profiles, and in consequence, the increasing the temperature and the heat transfer.

Small differences are observed when comparing velocity profiles between nanofluid and water in both cases. We also observe that the vertical velocity component is not affected by the type of nanofluid. This is the result of the use of the Brinkman formula (2005) to calculate the viscosity of the nanofluid which depends on the volume fraction.

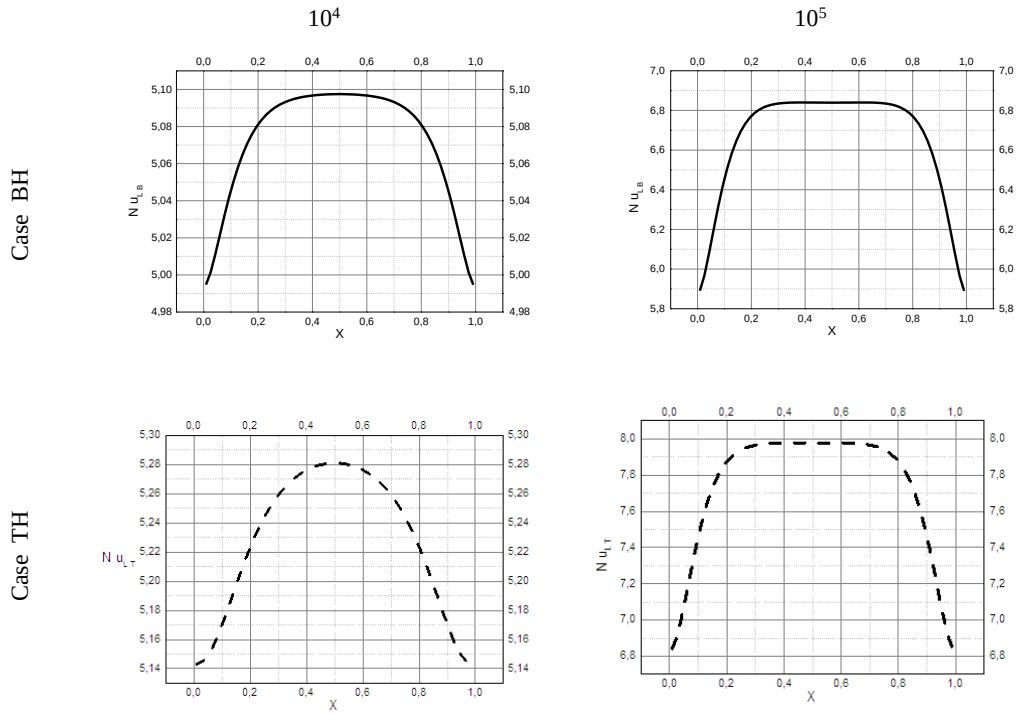

Fig. 9. The variation of the local Nusselt Number for two cases (BH and TH) and different Ra with Φ = 0.03.

The Nusselt number have a great significance dimensionless parameter in convective heat transfer study. The local values of the Nusselt number computed for the isothermal walls are shown as variations along the X-direction in Fig. 9 for Ra=10^4, 10^5, and the two configurations BH and TH. The figures show that the Nusselt number increases with increasing Rayleigh number as expected for two configurations BH and TH. In all these figures we observed a symmetric variation. The maximum values of the Nusselt number is achieved for Ra = 10^5 in the center of the cavity and becomes almost constant from the position X = 0.4 to X = 0.6 for the considered cases. We can also notice that the Nusselt number is important when the heated block is located at the top wall of the cavity in comparison with the other position, as it shows stronger thermal gradients on all sides of the heat source.

The variation of the average Nusselt number as a function of the heated block positions (Configurations BH and TH), for different Rayleigh numbers and different volumetric fraction values on each side of the block is presented in Tables 4 and 5. It is found that the Nu increases with the nanoparticles volume fraction for all the values taken by Ra. This increase is due to the improvement of the thermal conductivity of the nanofluid when the nanoparticles volume fraction increases.

It is also noted that for a given configuration (BH or TH), the greatest improvement in heat transfer can be achieved in the case of high Rayleigh number.

At low Ra, conduction plays an important role in heat transfer as nanofluids have a considerably higher thermal conductivity compared to base fluid, conduction is more efficient. As we increase the Rayleigh number value, the majority of the heat transfer occurs due to convection and thermal conductivity's role is reduced. Hence the use of nanofluids bring relatively lower heat transfer enhancement.

The same results were found by Oztop *et al.* (2008) for a 2D natural convection simulation and Ravnik (2010) for a 3D natural convection simulation.

We can also notice that the Nu_a increases with the Ra. It is also found from the table that when the heat source is located at the top wall of the cavity, the average Nusselt number reaches the maximum value for high Rayleigh number. In fact, as shown in Figs. 5 and 6, the isotherms relative to this position, in comparison with the other position, show stronger thermal gradients on all sides of the heated block.

5. CONCLUSION

In this paper, we examined the influence of the nanofluid type, the Rayleigh number and the heated block position (cases BH and TH) on the heat transfer induced by natural convection.

The results, illustrate a positive effect of the volume fraction and the Rayleigh number on the improvement of the heat transfer where:

- When the Rayleigh number increases, the buoyancy force becomes large, and therefore the maximum stream function of the pure fluid and the nanofluid increases.

Table 4 Comparison of the average Nusselt number in case BH between nanofluid (Water +Cu) and Water

Configuration BH								
Ra	Nu_a at the upper wall of the block							
	Φ = 0.00		Φ = 0.01		Φ = 0.02		Φ = 0.03	
10^3	2.674803		2.685183		2.686078		2.689767	
10^4	2.744839		2.757833		2.761487		2.785668	
10^5	3.921615		3.958614		3.978293		3.990647	
Ra	Nu_a at the Left wall of the block				Nu_a at the Right wall of the block			
	Φ = 0.00	Φ = 0.01	Φ = 0.02	Φ = 0.03	Φ = 0.00	Φ = 0.01	Φ = 0.02	Φ = 0.03
10^3	2.877913	2.898514	2.909374	2.925470	2.874500	2.895285	2.946319	2.962580
10^4	3.612638	3.664414	3.768949	3.806105	3.571496	3.585585	3.592352	3.641635
10^5	7.615639	7.647379	7.658842	7.710138	7.508012	7.539384	7.590548	7.621603

Table 5 Comparison of the average Nusselt number in Case TH between nanofluid (Water +Cu) and Water

Configuration TH								
Ra	Nu_a at the upper wall of the block							
	Φ = 0.00		Φ = 0.01		Φ = 0.02		Φ = 0.03	
10^3	2.802031		2.824931		2.868215		2.881838	
10^4	3.585978		3.615706		3.643685		3.691739	
10^5	4.586675		4.788817		4.795942		4.825593	
Ra	Nu_a at the Left wall of the block				Nu_a at the Right wall of the block			
	Φ = 0.00	Φ = 0.01	Φ = 0.02	Φ = 0.03	Φ = 0.00	Φ = 0.01	Φ = 0.02	Φ = 0.03
10^3	3.512937	3.533412	3.556022	3.586764	3.514801	3.527417	3.567755	3.589932
10^4	3.698326	3.727213	3.745205	3.765149	3.676893	3.690416	3.727776	3.737525
10^5	5.740019	6.393113	6.403784	6.462088	5.521361	6.260012	6.284083	6.350673

- The flow in the presence of nanofluid is stronger than that in the case of the pure fluid for Ra greater than 10^4.
- Small differences are observed when comparing velocity profiles between nanofluid and pure water in both cases. Where the vertical velocity component is not affected by the type of nanofluid.
- For Ra=10^5 the nanofluids velocity are higher than the those the pure water.
- The Nu increases with the Φ for different values the Ra, this is due to the thermal conductivity of the nanofluids .

The analysis of the results related to the heat transfer show that the copper-based nanofluid guarantees the best thermal transfer in the two considered configurations (BH and TH).

However, the optimum configuration, from the thermal and dynamical point of view, is the one with the heat source located on the upper wall (case TH). This position is the optimum choice in order to obtain the best heat transfer, because the thermal and dynamical transfers are influenced by the value of the buoyancy force which is favorable in the case of the configuration (TH).

REFERENCES

Abu-Nada, E. and H. F. Oztop (2009). Effects of inclination angle on natural convection in enclosures filled with Cu–water nanofluid. *International Journal of Heat and Fluid Flow*

Brinkman, H. C. (2005). The viscosity of concentrated suspensions and solution. Journal of Chemical Physics 20(65), 863-869. Choi, S. U. S. (1995). Enhancing Thermal Conductivity of Fluids with Nanoparticles, ASME. *Fluids Engineering Division*, 231, 99- 105.

Choi, S. U. S. (1995). Enhancing Thermal Conductivity of Fluids with Nanoparticles, ASME. *Fluids Engineering Division*, 231, 99-105.

Esmaeil, K. K. (2015). Thermophysical Properties Based Evaluation of Nanofluids Laminar Natural Convection Inside Square Enclosure. *J. Thermophys. Heat Transf* 29(1), 102–116.

Guiet, J., M. Reggio and P. Vasseur (2012). Natural convection of nanofluids in a square enclosure with a protruding heater. *Advances in Mechanical Engineering* 4, 167296.

Ho, .C. J., Liu W. K., Chang. Y. S. and C. C. Lin (2010). Natural convection heat transfer of

alumina-water nanofluid in vertical square enclosures: An experimental study. *International Journal of Thermal Sciences* 49(8), 1345–1353.

Ho, C. J., M. W. Chen and Z. W. Li (2008). Numerical simulation of natural convection of nanofluid in a square enclosure: Effects due to uncertainties of viscosity and thermal conductivity. *International Journal of Heat and Mass Transfer* 51, 4506–4516.

Hwang K. S, Ji-Hwan L, S. P. Jang (2007). Buoyancy-driven heat transfer of water-based Al2O3 nanofluids in a rectangular cavity. International *Journal of Heat and Mass Transfer* 50, 4003–4010.

Jou, R. Y. and S. C. Tzeng (2006). Numerical research of nature convective heat transfer enhancement filled with nanofluids in rectangular enclosures. *International Communications in Heat and Mass Transfer* 33, 727-736.

Khanafer, K., K. Vafai and M. Lightstone (2003). Buoyancy-driven heat transfer enhancement in a two-dimensional enclosure utilizing nanofluids. *International Journal of Heat and Mass transfer* 46, 3639-3653.

Lo, D. C., D. L. Young, K. Murugesan, C. C. Tsai and M. H. Gou (2007). Velocity–vorticity formulation for 3D natural convection in an inclined cavity by DQ method. *International Journal of Heat and Mass Transfer* 50, 479–491.

Mahmoudi, A., H. Shahi, M. Raouf, A. Honarbakhsh. (2010). Numerical study of natural convection cooling of horizontal heat source mounted in a square cavity filled with nanofluid. *International Communications in Heat and Mass Transfer* 37(8), 1135-1141.

Maxwell, James Clerk (1881). A treatise on electricity and magnetism. Clarendon press.

Oztop, H. F., E. Abu-Nada (2008). Numerical study of natural convection in partially heated rectangular enclosures filled with nanofluids. *International Journal of heat and Fluid Flow* 29, 1326-1336.

Patankar, V. S et D. Spalding, Brian. (1972). A calculation procedure for heat, mass and momentum transfer in three-dimensional parabolic flows. *International journal of heat and mass transfer* 15(10), 1787-1806.

Putra, N., W. Roetzel and S. K. Das (2003). Naturel convection of nanofluids. *Heat and Mass Transfer* 39, 775-784.

Ravnik, J., L. Škerget and M. Hriberšek (2010). Analysis of three-dimensional natural convection of nanofluids by BEM. *Engineering Analysis with Boundary Elements* 34(12), 1018-1030.

Sannad, M., A. Btissam, B. Lhousin and D. Hicham (2016). Numerical Study of Natural Convection in a Three-dimensional Cavity Filled with Nanofluids. *IJCSI International Journal of Computer Science Issues*.

Santra, A. K. , S. Swarnendu and N. Chakraborty (2008). Study of heat transfer augmentation in a differentially heated square cavity using copper–water nanofluid. *International Journal of Thermal Sciences* 47, 1113–1122.

Sheikhzadeh, G. A., M. Dastmalchi and H. Khorasanizadeh (2013). Effects of nanoparticles transport mechanisms on Al2O3–water nanofluid natural convection in a square enclosure *International Journal of Thermal Sciences* 66, 51–62.